19 cy Recd
19 cy for DCRS Distr.

HEDL-TME 71-57
APRIL 1972

MASTER

ANALYSIS OF FTR PHASE B CRITICAL EXPERIMENTS PART-3 DOPPLER EFFECTS IN ZPR-3, ASSEMBLY 51

HANFORD ENGINEERING DEVELOPMENT LABORATORY
UNITED STATES ATOMIC ENERGY COMMISSION

CONTRACT AT(45-1)-2170

HEDL-TME 71-57
APRIL 1972

ANALYSIS OF FTR PHASE B CRITICAL EXPERIMENTS PART-3 DOPPLER EFFECTS IN ZPR-3, ASSEMBLY 51

R.A. Bennett
W.R. Young

HANFORD ENGINEERING DEVELOPMENT LABORATORY

UNITED STATES ATOMIC ENERGY COMMISSION

CONTRACT AT(45-1)-2170

TABLE OF CONTENTS

LIST OF ILLUSTRATIONS

List of Illustrations (Cont'd)

LIST OF TABLES

ANALYSIS OF FTR PHASE B CRITICAL EXPERIMENTS

PART-3

DOPPLER EFFECT IN ZPR-3, ASSEMBLY 51

W. R. Young

R. A. Bennett

I. INTRODUCTION

The Fast Flux Test Facility (FFTF) Critical Experiments Program is providing experimental data for evaluation of calculational methods being used in the design of the Fast Test Reactor (FTR) and experimental verification of the design of the FTR. Several sets of experiments were performed in ZPR-3, Assembly 51 by Argonne National Laboratory personnel in cooperation with FFTF personnel. The experiments included measurements of critical mass and edge-drawer reactivity worths, spatial distributions of reaction rates, small sample reactivity worths, distributed sodium voiding reactivity worth, large sample core reactivity worths, fuel compaction and fuel movement reactivity worths, fission rate ratios, neutron spectra, and Doppler effects. This report presents the results of an analysis of the Doppler effects experiments. The results and analysis of the other experiments were reported earlier[1,2].

These analyses were made with a cross section set[3] that is based on a modified version of the ABBN 26 energy group cross sections[4]. Effects of crystalline binding were not included in this analysis. Indications are that accounting for crystalline binding effects will reduce the calculated Doppler effects. The reductions are expected to be non-linear, with the greatest reductions occurring at lower temperatures.

II. SUMMARY

Experimental evaluation of the accuracy of the calculated value of the Doppler constant of the FTR is a desired goal to be reached prior to final design and construction of FTR. Ideally, such experiments should involve the heating of an entire FTR mockup. Further, it would be necessary to separate the Doppler effects from other temperature effects, specifically expansion. Such a procedure has not been achieved successfully in existing fast reactor zero power test facilities to date. Small sample Doppler experiments constitute the only known alternative and are being used in this program. The extrapolation of results obtained from such small sample experiments to a reactor Doppler constant is at best difficult and will depend to a great extent upon success achieved in these early pilot experiments.

The specific goals of these experiments are, therefore, to establish:

1. The experiment-theory correlations on small sample Doppler constants in an FTR-like system.
2. Some experimental measure of the spatial dependence of the small sample Doppler constant as well as the corresponding spatial experiment-theory correlations.

Within the time limitations imposed in the early Phase B[5] portion of the FTR Critical Experiment twelve Doppler experiments were performed using a single UO_2 Doppler sample on the core midplane at the core axis, r = 0, midway out in the core, r = 22.2 cm, and near the core boundary, r = 33.3 cm.

At each location, the Doppler reactivity effect of the sample, due to temperature changes from 300°K to 500°K, 300°K to 800°K, and 300°K to 1100°K, was determined using a nickel buffer sleeve on the Doppler sample. For the same temperature increments, but with a stainless steel buffer, the experiments were repeated at r = 0.

Calculation to experiment ratios of the Doppler effects, c/e values, for a 300°K to 1100°K temperature change ranged from 1.13 at the core center to 0.836 at the core edge with a nickel buffer and are as large as 1.27 at the core center with a stainless steel buffer.

Statistical analyses[6] of the experimental data and corresponding calculated results indicate that

1. The root mean square difference between calculated reactivity changes and experimental changes is 0.0086, which is consistent with the quoted experimental uncertainties. One may then infer that the calculational procedure correctly models the temperature dependence of the Doppler effect.
2. The calculated changes underestimate the experimental changes on the average by approximately 6%, which may be taken as a systematic bias in the calculational procedure.
3. The calculational procedure has a radially dependent negative bias, e.g. at r = 22.2 cm the calculated values should be reduced by -0.0014 and at r = 33.3 cm they should be reduced by -0.0373.

Finally the experimental results may be predicted by the expression;

$$E = A(r) + 1.06\ C$$

where E = the experimental result

A(r)= the radially dependent correction function, and

C = the calculated result.

While this analysis indicates trends and biases, it has been concluded that the calculational model is sufficiently adequate to yield small sample Doppler effect estimates with an uncertainty in the neighborhood of ±25% for all spatial positions. This is not inconsistent with the Recommended Expected Nuclear Design Uncertainty presented in the LMFBR Liquid Metal Fast Breeder Reactor Program Plan[7].

One may further conclude that Doppler coefficients for an entire reactor are calculated even better because the c/e values have a spatial trend from greater than unity at the core center to less than unity at the core boundary, thus producing compensating effects in calculated values.

Finally, these data have been used to estimate a bias of-10% in the calculated value of the Doppler coefficient for Assembly 51 i.e., the value is underestimated by 10% using these methods and cross sections. It is expected that calculations on the FTR will not be significantly more in error than indicated here. Follow-on FTR Engineering Mockup Experiments will be used to validate this expectation.

In this work the original reference cross section set for FTR design was used[3]. Additional analyses are now underway using the reference cross section set being employed in the final design of FTR.

III. DESCRIPTION OF EXPERIMENTS

3.1 Description of Experimental Test Bed: ZPR-III Assembly 51

A detailed description of ZPR-III Assembly 51 has been reported by the experimentalists and has also been included in an earlier analysis report[1]. To recapitulate, the assembly was a completely reflected irregular right cylindrical core. Detailed areal profiles are shown in Figures 1 through 6. Each matrix cell of each of the figures represents

a ZPR-3 matrix tube, a drawer, and its contents. Each matrix cell is 2.178 inches wide and 2.182 inches high.

The core cell for the assembly consists of two matrix tubes filled with plates arranged as shown in Figure 7. Details of the reflector cells, plutonium spiked safety drawers, and control drawers are given in Reference 1.

The core composition is 36 vol% fuel, 36 vol% sodium, and 25 vol% stainless steel. The radial reflector was composed of 16 vol% sodium, 12 vol% stainless steel, and 61 vol% nickel. The axial reflector had approximately 41 vol% sodium, 17 vol% stainless steel, and 31 vol% nickel. Exact homogenized compositions of the various zones of the assembly are given in Table 1.

Detailed atom densities for the drawers are given in Reference 1. Nominal dimensions of the equivalent right circular cylindrical assembly are: core height 86.520 cm, and core radius 33.239 cm, as shown in Figure 8. These dimensions conserve the core volume of Figure 1. Axial and radial reflectors are nominally 30 cm thick.

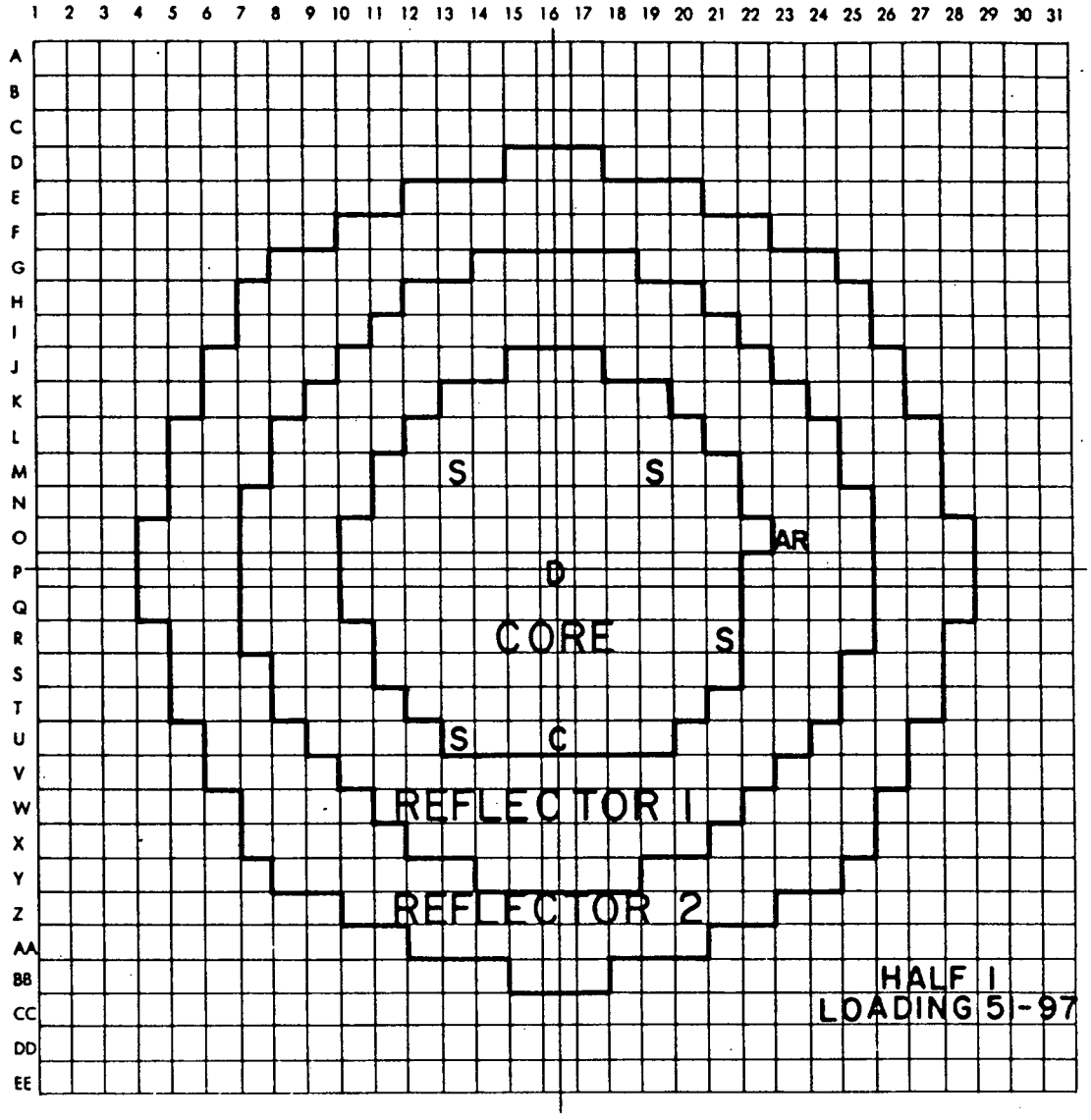

C= CONTROL ROD S= SAFETY ROD AR= AUTO ROD D= DOPPLER

Figure 1. Doppler Experiment Loading, Assembly 51

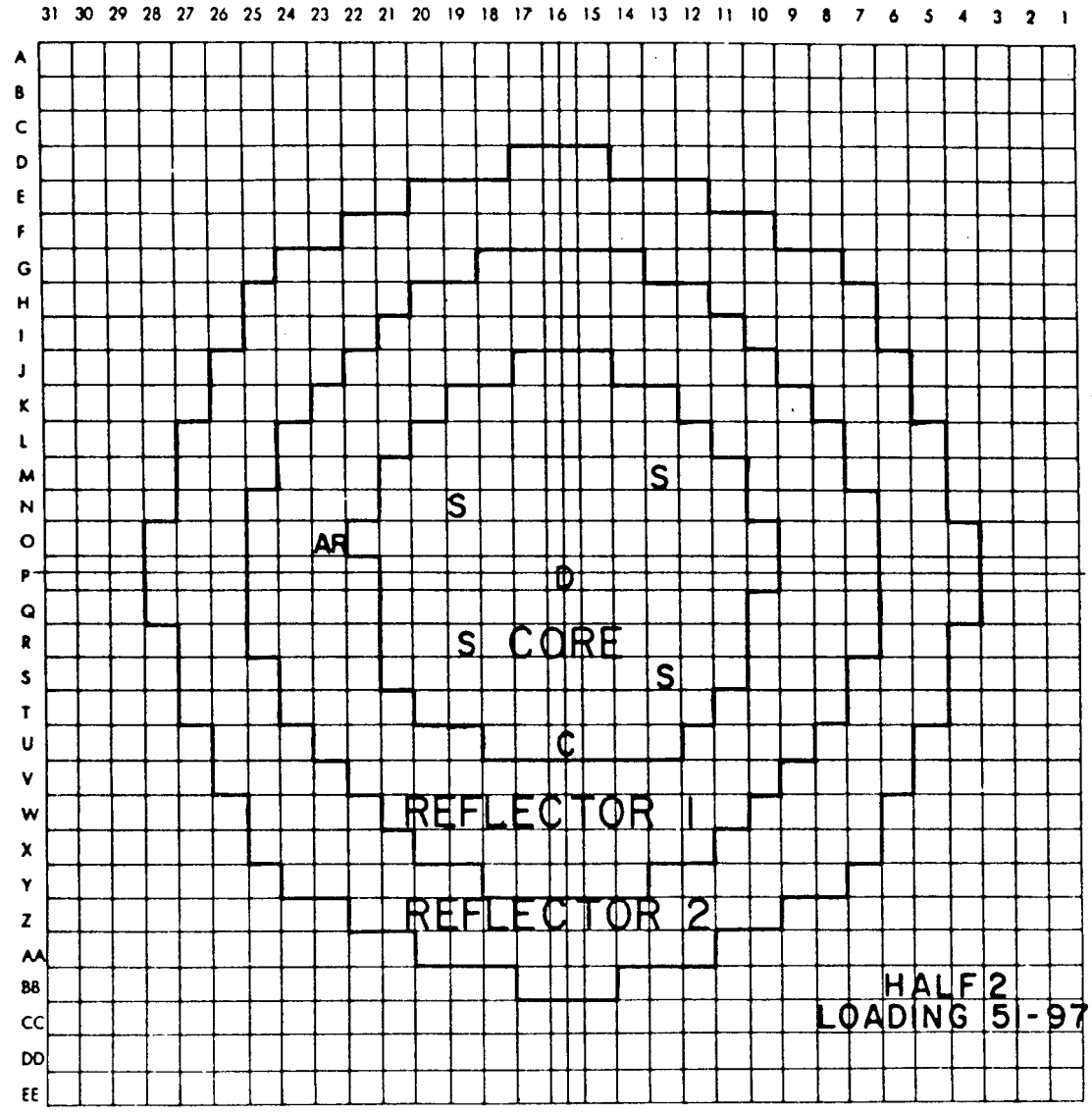

C = CONTROL ROD S = SAFETY ROD AR = AUTO ROD D = DOPPLER

Figure 2. Doppler Experiment Loading, Assembly 51

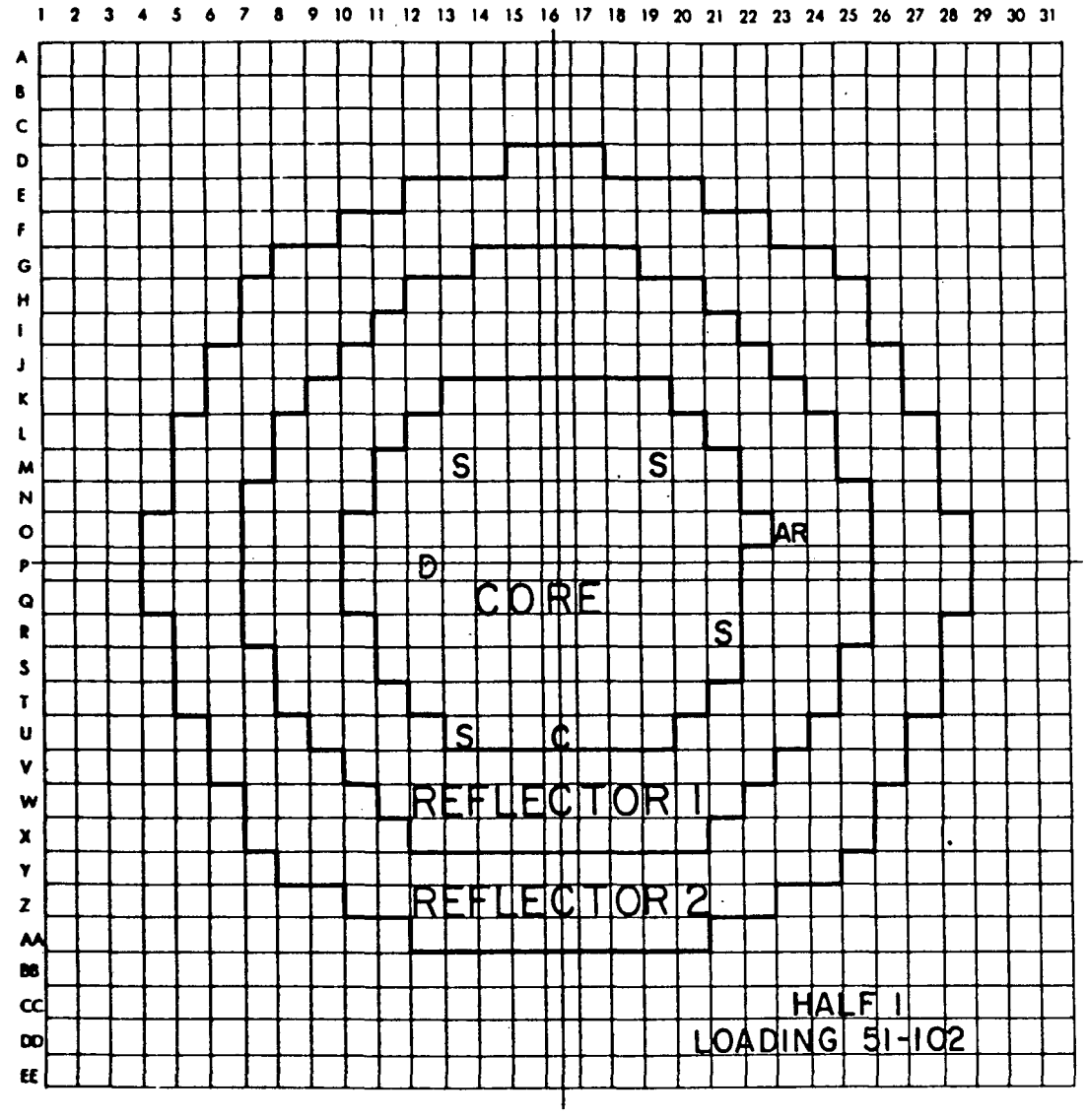

C = CONTROL ROD S = SAFETY ROD AR = AUTO ROD D = DOPPLER

Figure 3. Doppler Experiment Loading, Assembly 51

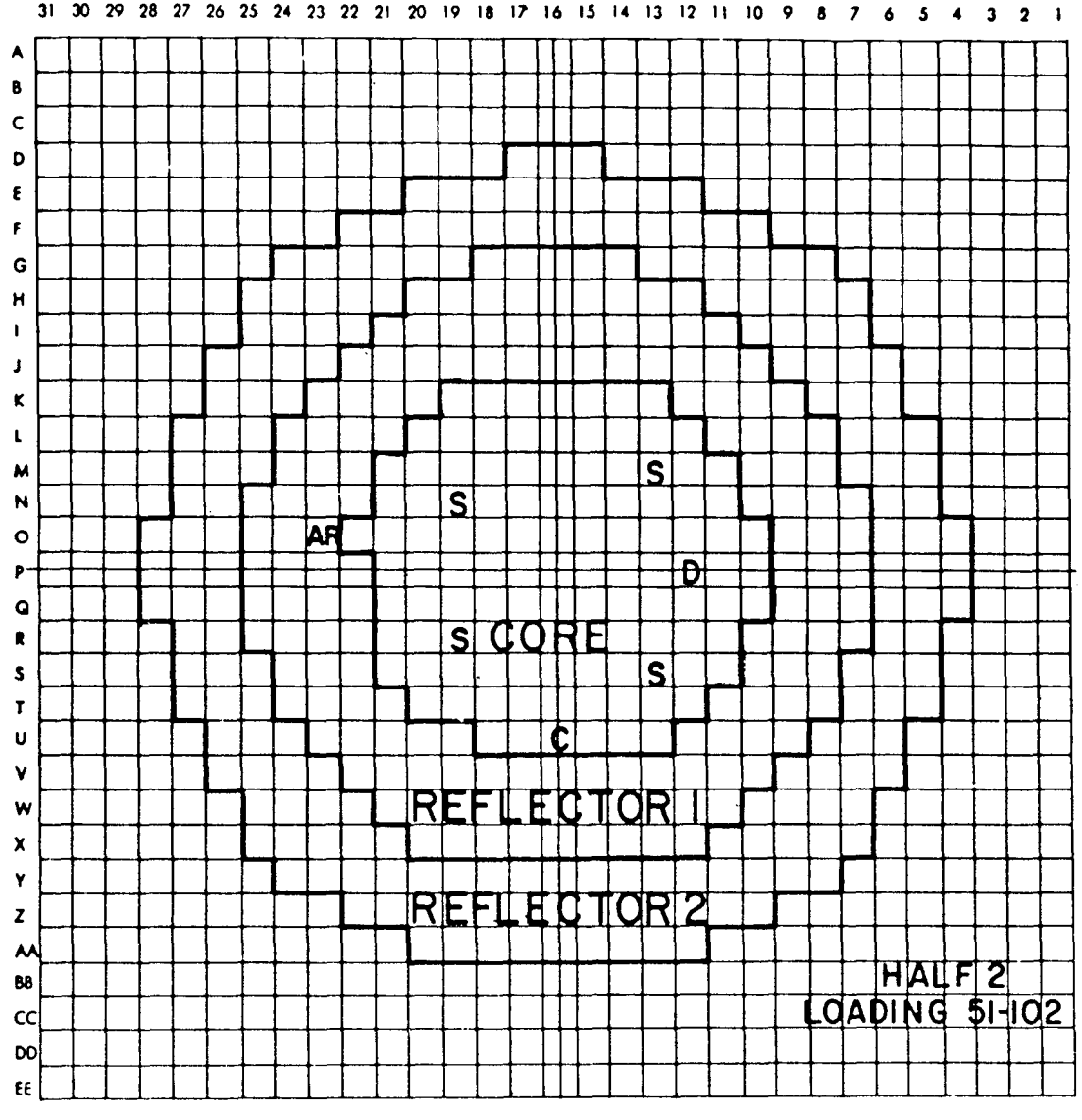

C = CONTROL ROD S = SAFETY ROD AR = AUTO ROD D = DOPPLER

Figure 4. Doppler Experiment Loading, Assembly 51

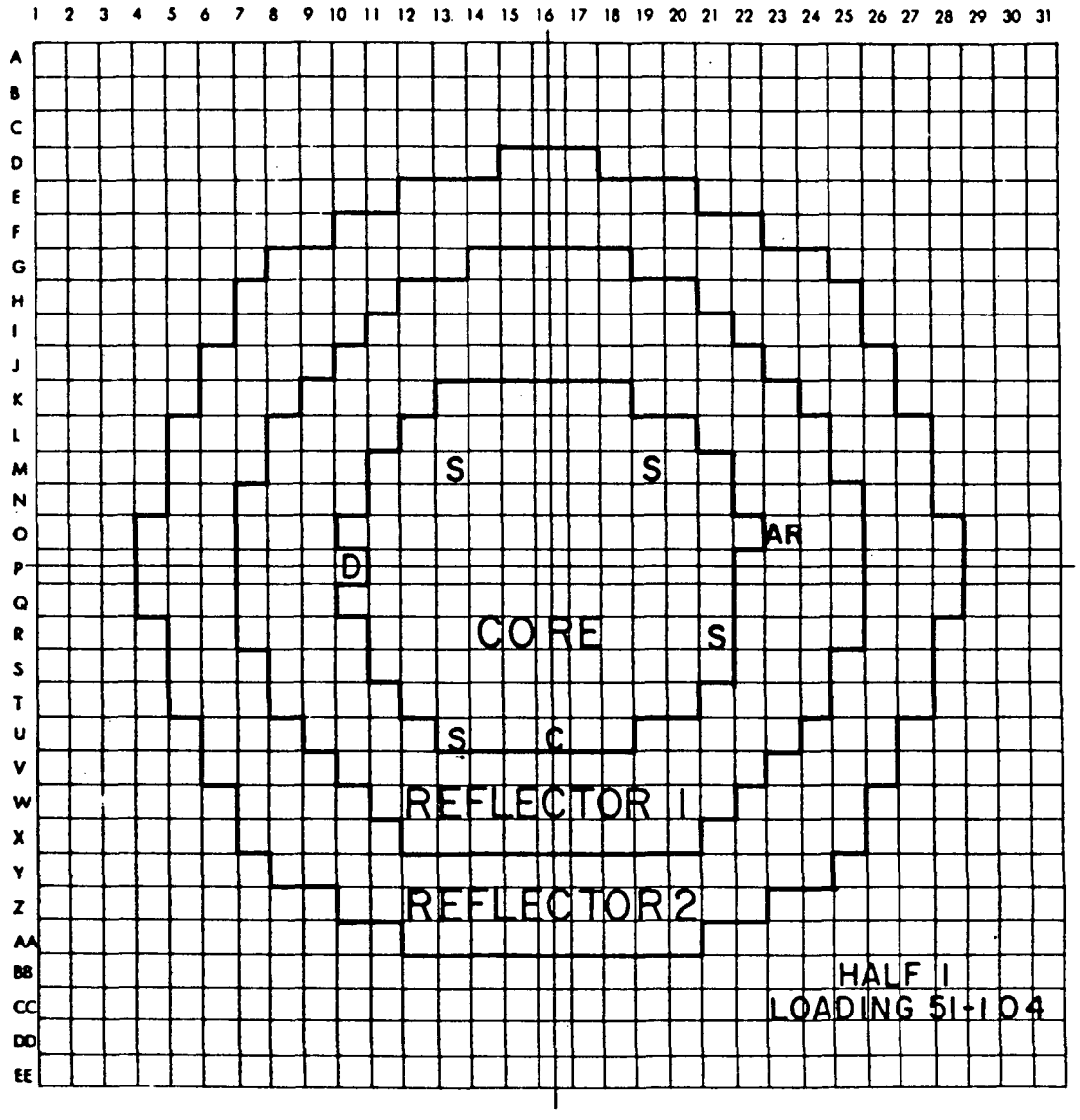

C = CONTROL ROD S = SAFETY ROD AR = AUTO ROD D = DOPPLER

Figure 5. Doppler Experiment Loading, Assembly 51

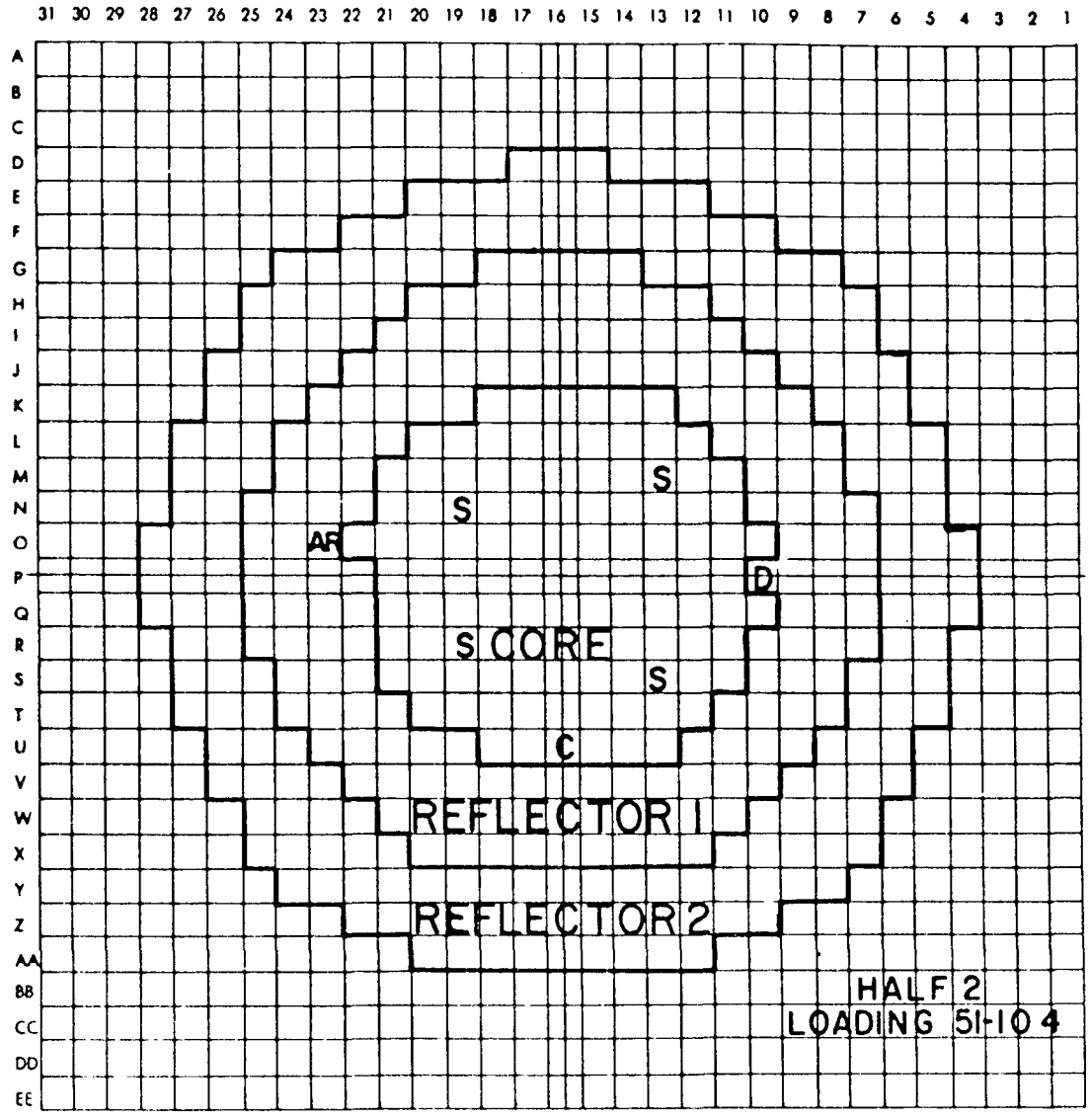

C = CONTROL ROD S = SAFETY ROD AR = AUTO ROD D = DOPPLER

Figure 6. Doppler Experiment Loading, Assembly 51

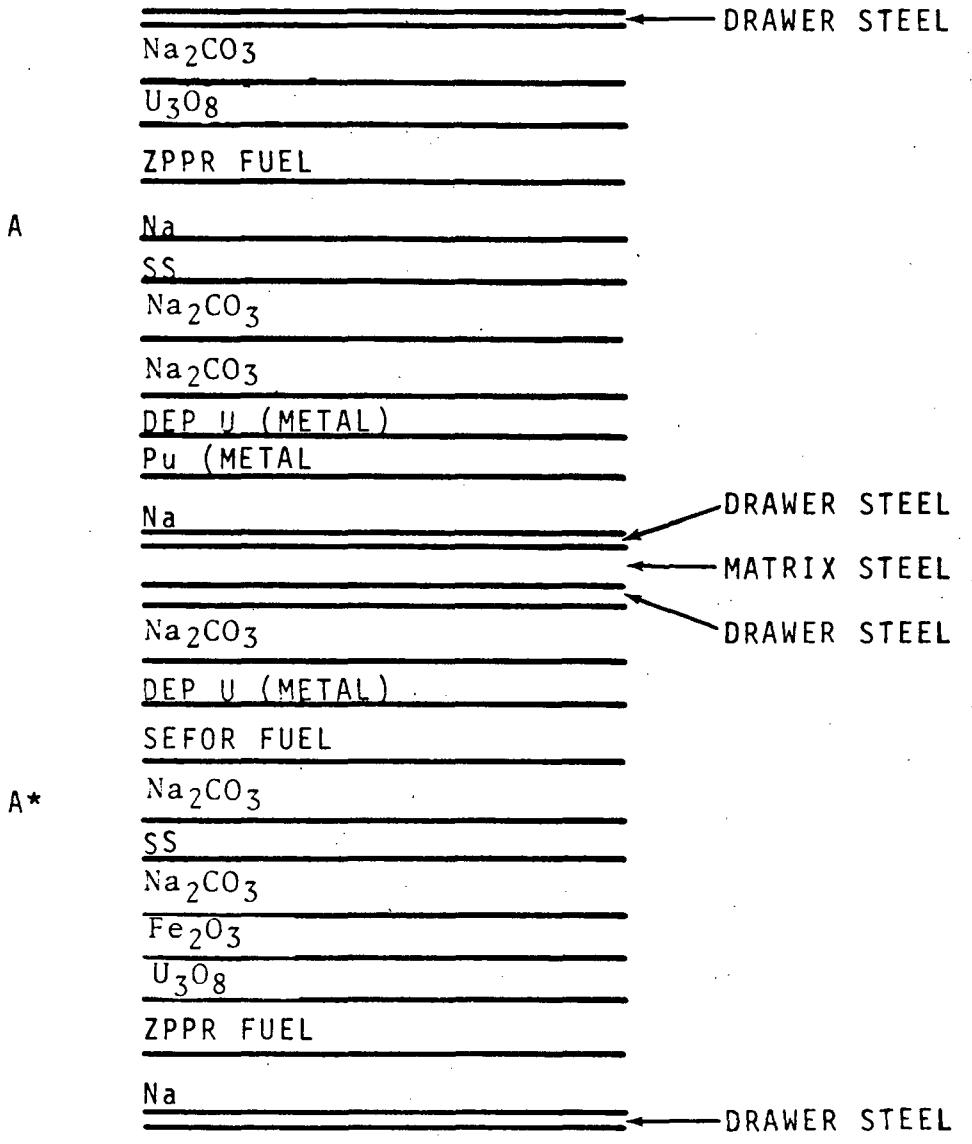

Figure 7. Core Cell Loading for ZPR-3, Assembly 51

TABLE I
ATOM DENSITIES FOR ZPR-III ASSEMBLY 51 DOPPLER EXPERIMENTS

Atoms/cc x 10^{-22}

Zone	Pu-239 -241	Pu-240 -242	U-235	U-238	Mo	Na	C	O	Al	Fe	Cr	Ni	Mn	Si
Core	.1736	.0173	.0015	.7007	.0328	.9256	.3113	1.2790	.0055	1.5620	.3657	.1600	.0153	.0179
Radial Reflector I						.4160				.7605	.1870	5.6400		.0090
Radial Reflector II						1.0321				7.4860	.1150	.0480		.0060
Axial Reflector						1.0321				1.0426	.2583	2.8926	.0182	.0126
Ni-SS Region-Ni Buffer*										.4644	.1213	2.3870		
Ni-SS Region-SS Buffer*										3.6434	.9513	.3747		
Nickel												9.1300		
UO_2 Rod			.0100	1.5600				3.1400						
Heater & Insulation Simulation										.6510	.1700	.6070		

* Material in Doppler Matrix Tube Behind Doppler Sample.

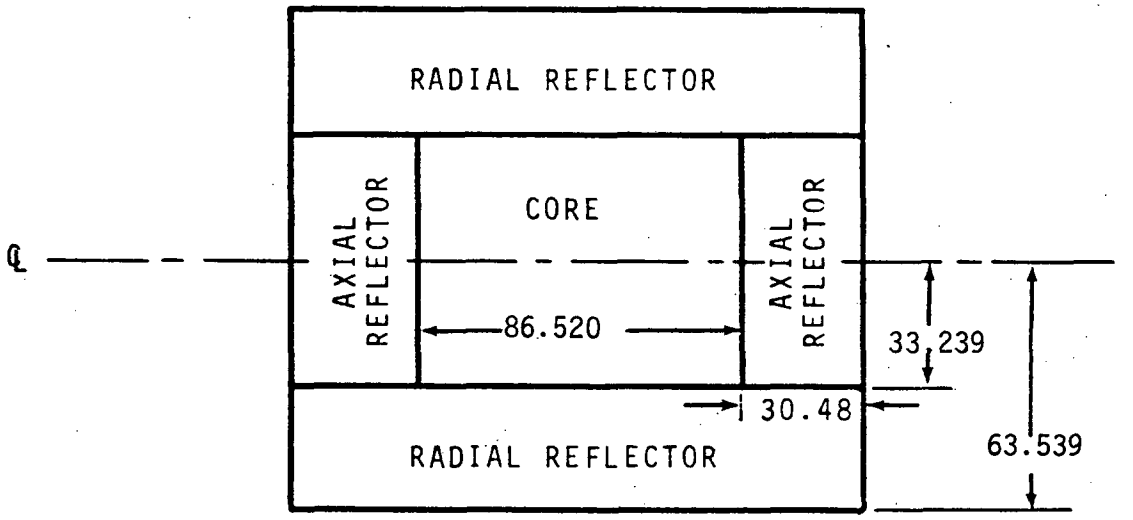

FIGURE 8. Assembly 51 Volume Equivalent Right Circular Cylinder

3.2 Doppler Experiments, Description and Results

Doppler samples were positioned on the midplane of Assembly 51 at radii of 0, 22.2, and 33.3 cm. Doppler effects were induced by heating a small cylindrical uranium dioxide sample over the temperature range of 300°K to 1100°K. Reactivity changes due to the sample temperature changes were fractions of an inhour ($\sim 10^{-6}$ $\Delta k/k$) and were measured[8] by an oscillator technique developed at ANL[9].

The Doppler sample was a 137.2 gram, 1/2 inch diameter, 6 inch long, right circular cylinder. Temperature changes were accomplished through the use of an annular heating element immediately adjacent to the sample. This assembly and heater is shown in Figure 9. As shown in the figures, the sample and heater were contained in a single matrix tube lined with a nickel or stainless steel buffer annulus 3/8 inch thick.

This buffer annulus was employed to reduce the so-called hot-cold resonance interaction effect resulting from the relative proximity of the heated uranium in the sample to the ambient uranium in the reactor core. As discussed by Lewis and Johnson[10] and Hwang and Miller[11], the presence of cold uranium near a uranium Doppler sample will increase the experimentally observed Doppler reactivity effects, induced by heating the sample, by depressing the energy distribution of neutrons at resonance energies more severely than on resonance wings. This reduces the extent to which resonance reaction rates decrease due to Doppler broadening of the resonances.

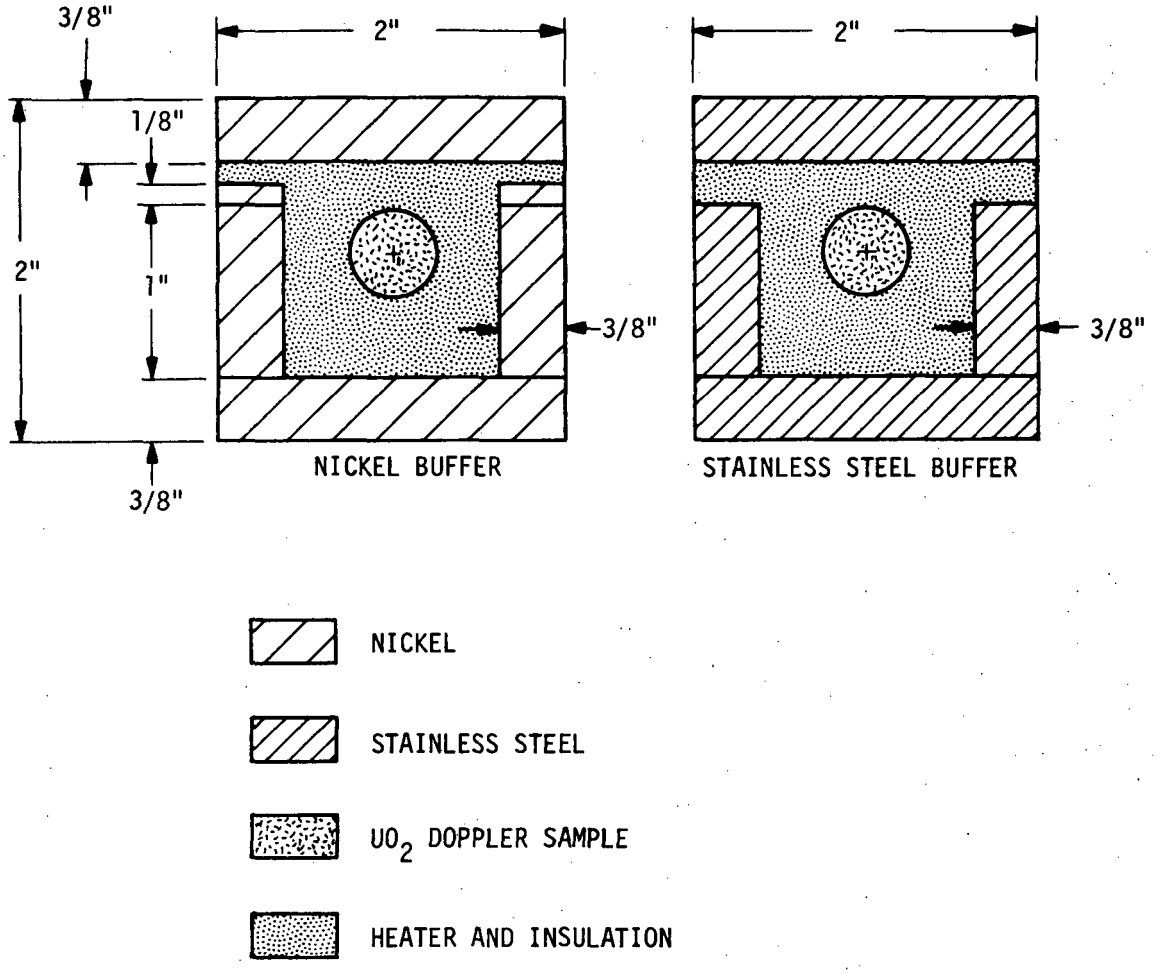

Figure 9. Doppler Cells in ZPR-3, Assembly 51, Core Midplane.

The addition of the buffer tends to eliminate this effect by thermalization of neutrons and hence the filling in of the resonance flux depressions in the incident flux. Thus, the observed Doppler effects would decrease. Simultaneously, however, the thermalization increases the low energy flux incident on the sample from the core and this increases the observed Doppler effects. For the 3/8 inch buffer used here. the hot-cold resonance interaction is reduced from as much as 20% down to 2%. The flux perturbation increases the observed effects by a corresponding amount. Hence, the observed effects are expressed to be larger than the specific Doppler worths for a heated core.

Thermal expansion of the samples has been virtually eliminated by design of the sample[10].

Reactivity changes were actually measured for temperature changes in the sample of 300 to 500°K, 300 to 800°K, and 300 to 1100°K at each of the three radial locations. The nickel buffer was used in all locations while the stainless steel buffer was used only at the center. The experimental results are given in Table II. Uncertainties quoted in Table II include the random statistics of the oscillator technique as well as a 1% uncertainty in auto rod calibration. As mentioned above, expansion effects are negligible.

TABLE II

EXPERIMENTAL RESULTS OF DOPPLER EFFECTS MEASUREMENTS[8]

Location	Distance from Axis, cm	Buffer	Sample Worth, Ih 300°K	Reactivity Change in Heating from 300°K, Ih to 500°K	to 800°K	to 1100°K
P16	0	Nickel	-4.27 ±0.09	-0.1315±0.007	-0.2745±0.008	-0.3857±0.009
P16	0	SS	-3.23 ±0.03	-0.1019±0.005	-0.2208±0.006	-0.3068±0.007
P12	22.2	Nickel	-1.096±0.0011	-0.0846±0.0066	-0.1516±0.007	-0.2258±0.006
P10	33.3	Nickel	+0.187±0.002	-0.0728±0.0054	-0.1451±0.006	-0.1989±0.006

Before proceeding to discussions of the experiment-theory correlations of these data and corresponding calculated values it is of interest to obtain an analytic fit to the data. Ideally one would like to fit the function

$$T^{\alpha}\frac{dk}{dT} = b$$

However, the data are far too sparse to yield a satisfactorily significant statistical uncertainty in α. The quantity α has therefore been set equal to unity and the fitting was done with the function

$$T\frac{dk}{dT} = b$$

or $$\Delta k = b \ln\left(T/T_o\right)$$

where T_o = the initial temperature of the Doppler sample

and T = the final temperature of the Doppler sample.

The data and the fitted curves are shown in Figures 10, 11, 12, and 13. Values of the coefficients of the fitted curves are

SPATIAL POSITION (CM)	b Ih	Buffer
0	-0.2876 ± 0.0214	Nickel
22.2	-0.1667 ± 0.0154	Nickel
33.3	-0.1540 ± 0.0059	Nickel
0	-0.2291 ± 0.0184	SS

where the uncertainties are standard deviations.

Figure 11 shows that the 800°K data point lies about 2σ from the best fitted line which suggests that it may be in error, experimentally. This point is discussed later in the Analysis Section where calculated Doppler effects are compared with measured values.

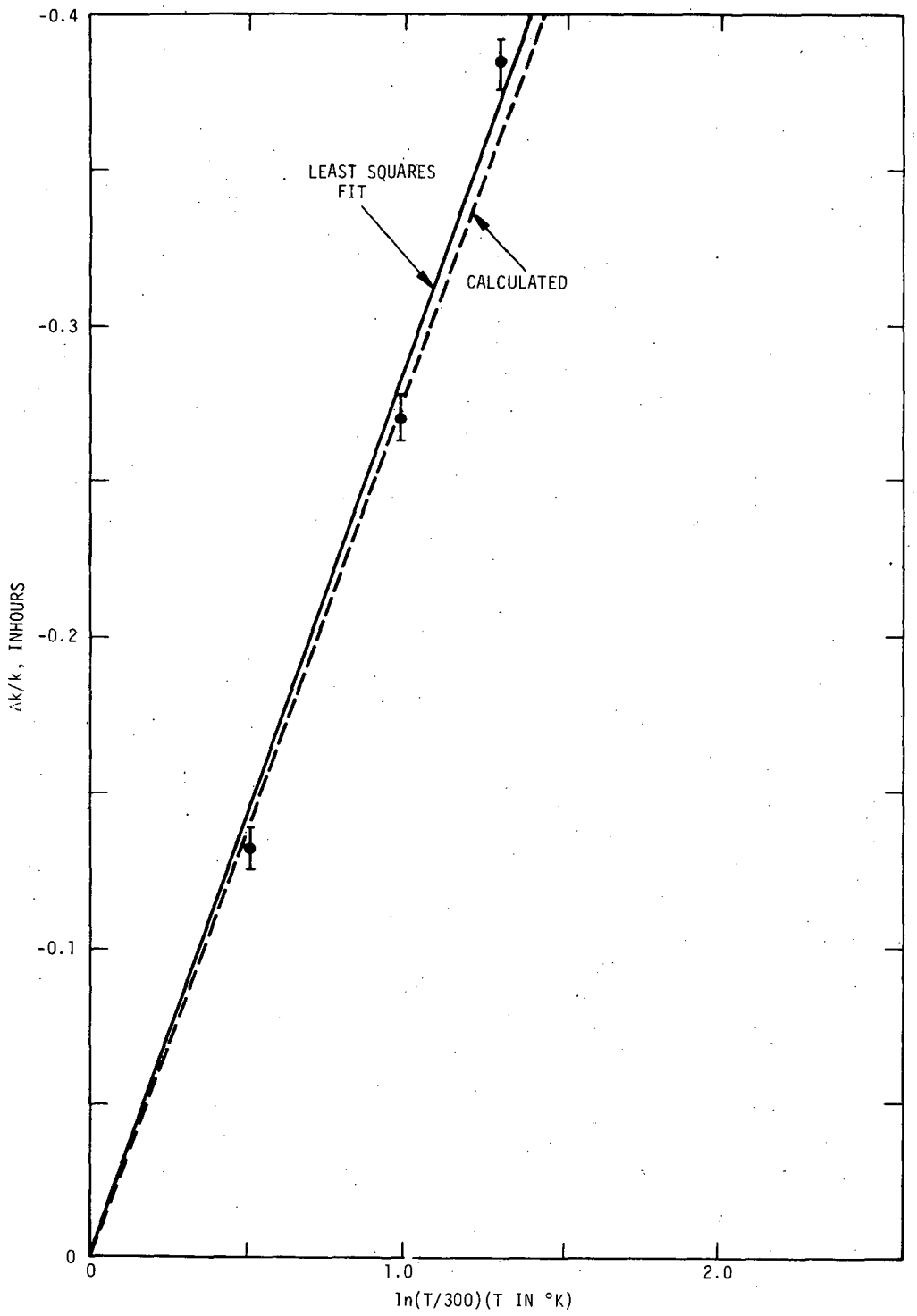

Figure 10. Temperature Dependence of Doppler Sample Worth, r=0 Nickel Buffer.

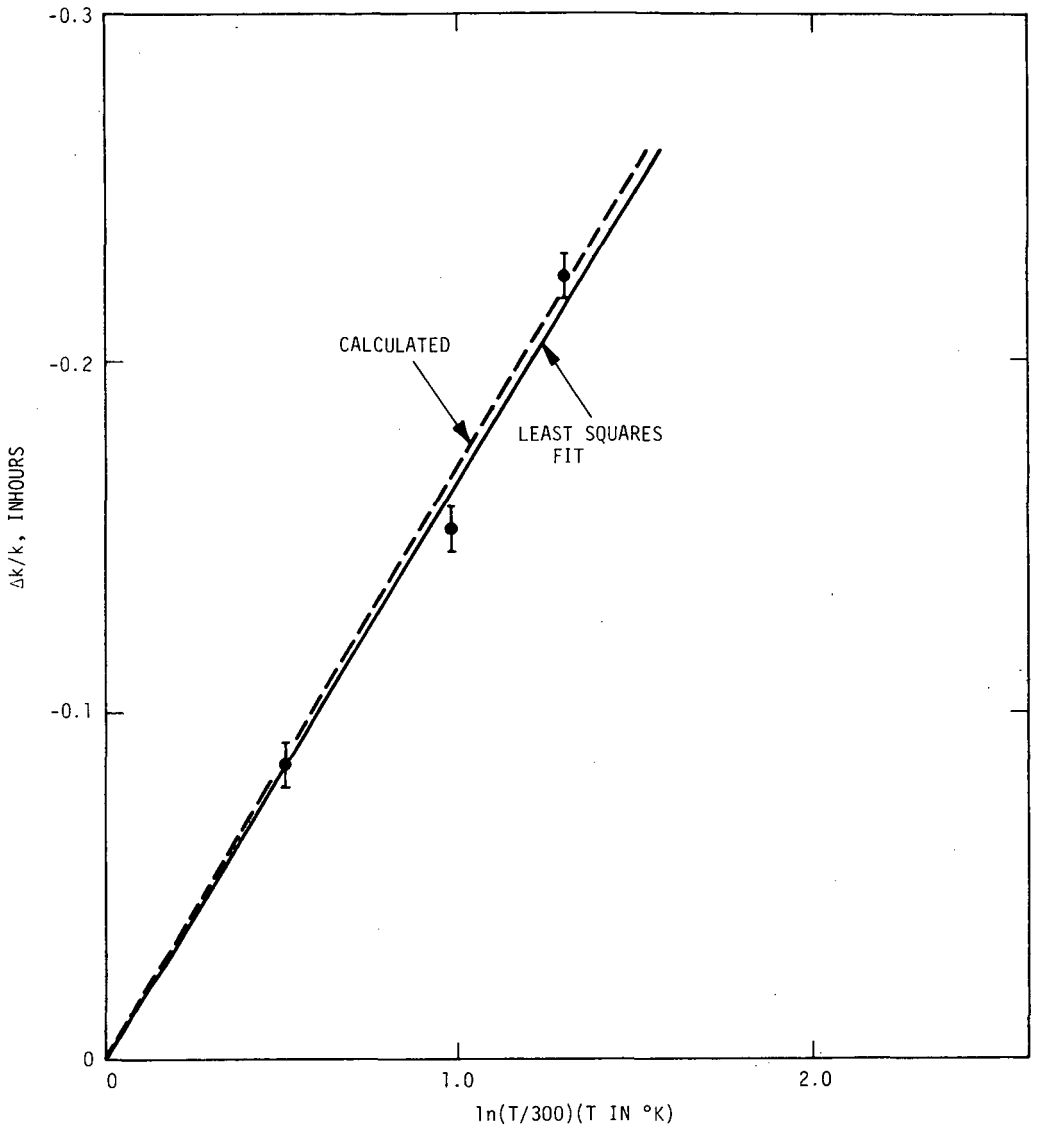

Figure 11. Temperature Dependence of Doppler Sample Worth, r=22.2 cm Nickel Buffer.

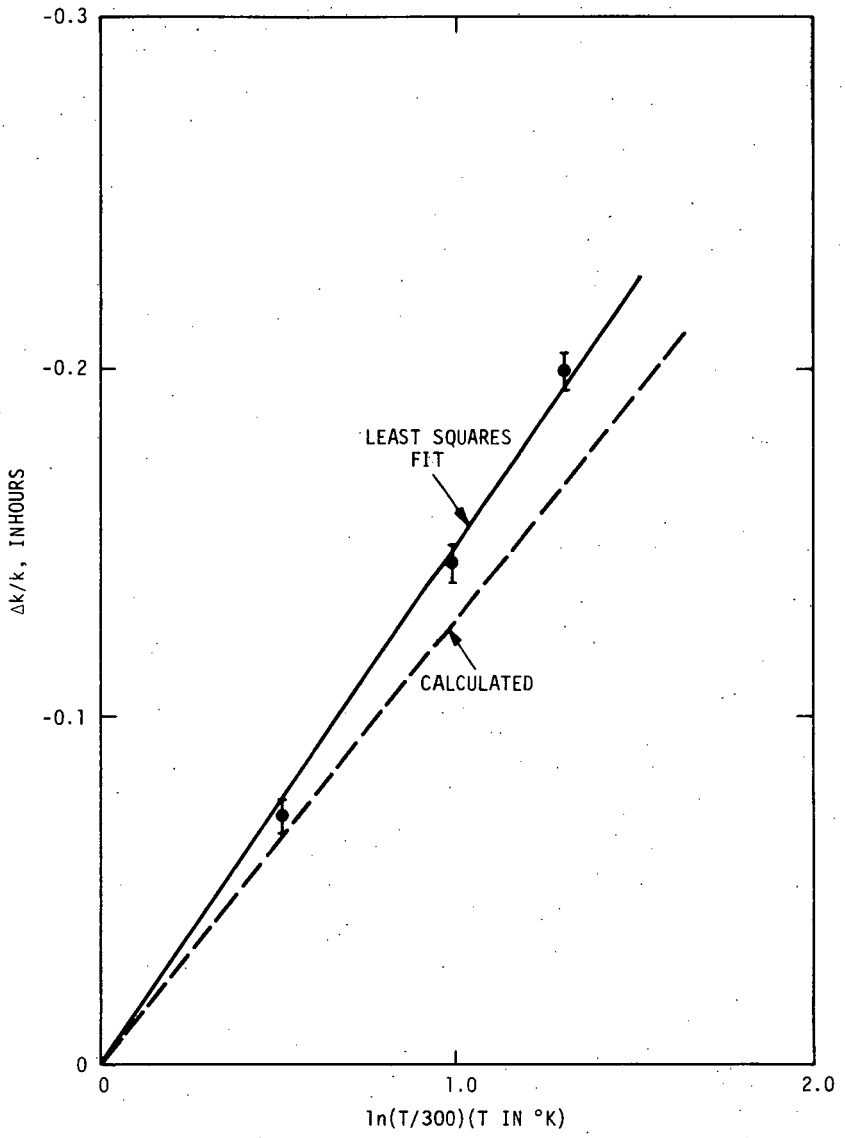

Figure 12. Temperature Dependence of Doppler Sample Worth, r=33.3 cm Nickel Buffer

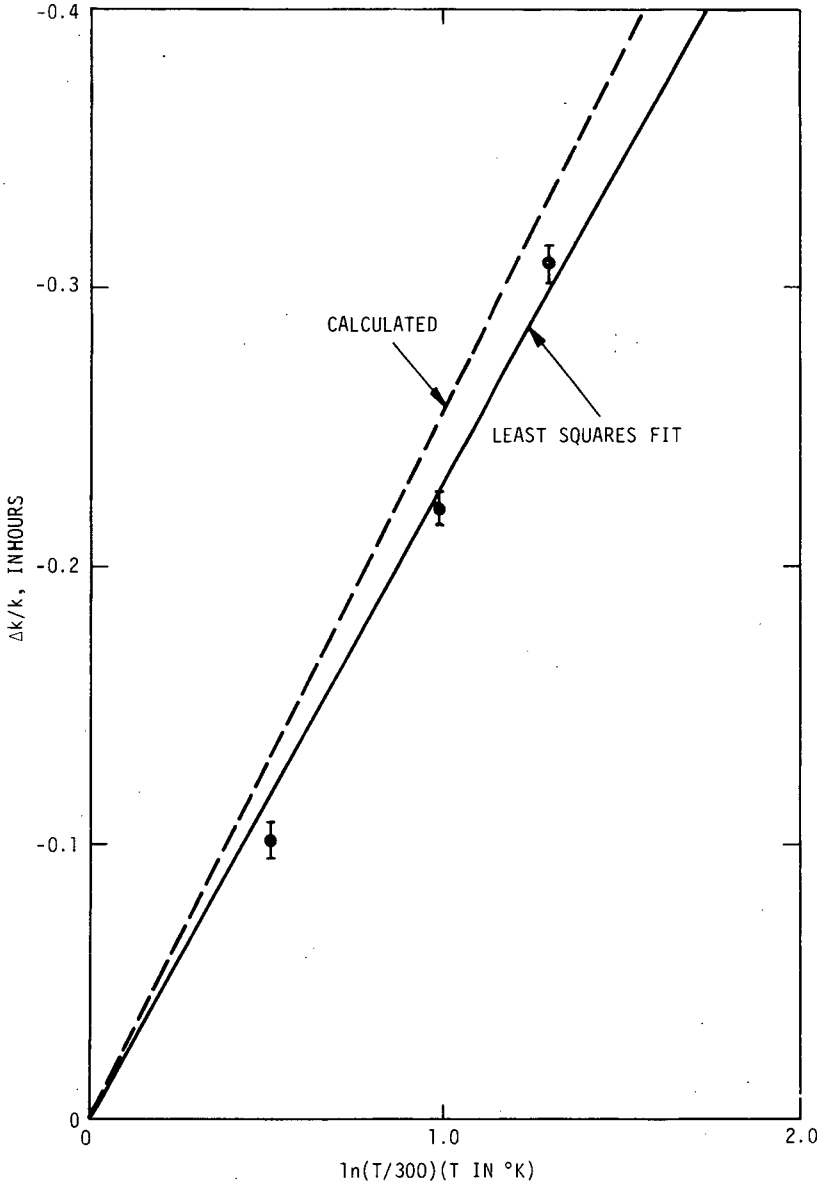

Figure 13. Temperature Dependence of Doppler Sample Worth, r=0 Stainless Steel Buffer

IV. ANALYSIS AND COMPARISONS WITH EXPERIMENT

4.1 Analytical Methods

Analyses of Doppler effects experiments were done with the following computer programs:

Program	Ref.	Description
1 DX	12	Multigroup 1D diffusion theory
DTF IV (modified)	13	Multigroup 1D transport theory
2DB	14	Multigroup 2D diffusion theory
PERT-IV	15	2 dimensional 1st order perturbation theory

Cross sections[3] employed in these analyses were those prepared for the preliminary design of FTR and early analyses of FFTF Critical Experiments. They are a modified version of the ABBN 26 group set[4]. Cross section processing and analyses proceeded as follows:

4.1.1 Doppler Cell Cross Sections

In subsequent reactor calculations, to obtain real and adjoint fluxes for perturbation calculations of Doppler sample worths as a function of temperature, the Doppler cell was represented as a homogeneous lump. This significantly reduced the required cell mesh detail and calculational expense. Cross sections for this homogenized lump were first resonance self-shielded using the Bell correction[16], an integral part of the Program 1DX.

Specifically, resonance self-shielding factors are tabulated in the basic cross section library for each isotope, k, and each energy group as a function of temperature, T, and the total potential cross section per atom, $\sigma_{T,k}$, where

$$\sigma_{T,k} = \frac{\Sigma_o}{N_o^K} + \frac{\Sigma_1 V_1}{N_o^K V_o} \cdot \frac{1}{1 + X \Sigma_i} \qquad (4.1)$$

and

$X = 4 (V_o + V_1)/S_o$ = Heterogeneity constant, cm

V_o = volume of fuel region, cm^3

V_1 = volume of diluent region, cm^3

S_o = surface area of fuel region, cm^2

N_o^k = atom density of isotope k in the fuel region

Σ_o = macroscopic total cross section in the fuel excluding isotope k, cm^{-1}

Σ_1 = macroscopic total cross section in the diluent region, cm^{-1}

$\Sigma_1' = V_1\Sigma_1/V_o + V_1)$, cm^{-1}

The Bell correction enters the calculation through the total potential cross section, Equation 4.1, as the input constant X. The Doppler cell diluent volume, V_1, was assumed to extent outward from the UO_2 pin surface to an infinite cylindrical surface where the resonance neutrons, energy groups 10 through 21, have a calculated vanishing derivative. This surface, 1.75 cm from the UO_2 pin axis, was found from a DTF-IV, S-8 calculation. A plot of the calculated total resonance flux is given in Figure 14. Using the UO_2 pin radius, 0.636 cm, and an outer cell boundary of 1.75 cm, gives a value of 9.631 cm for X.

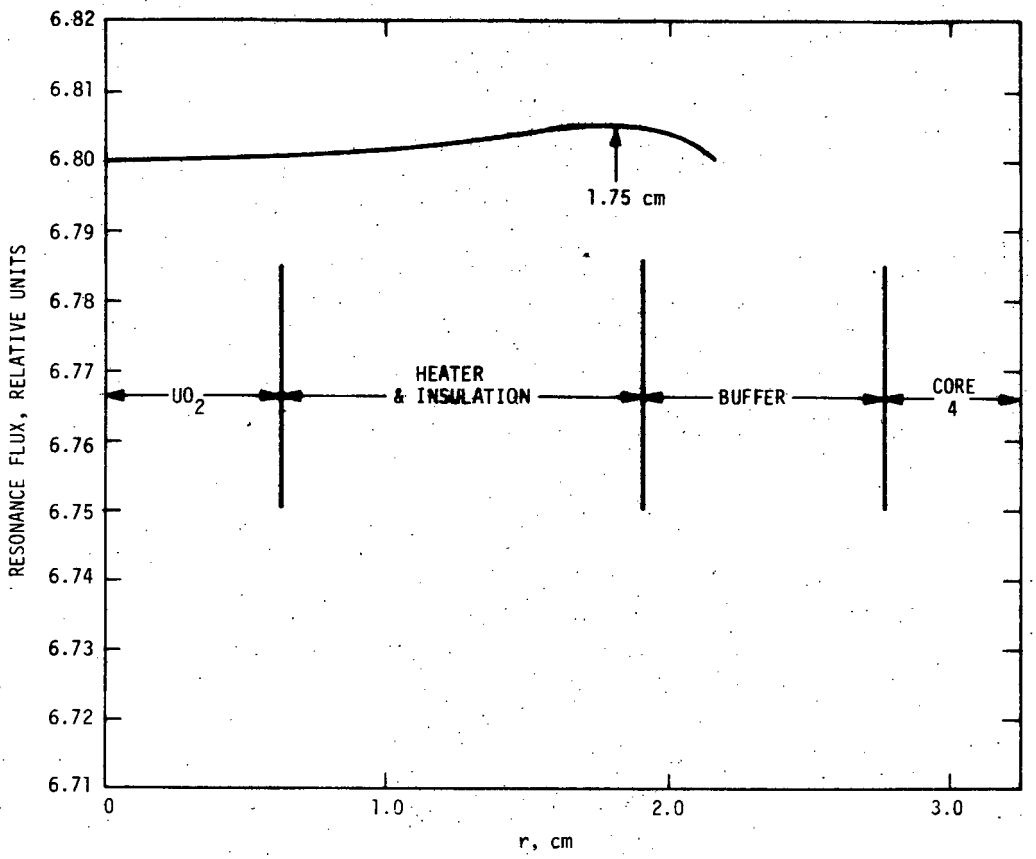

Figure 14. Resonance Flux in Doppler Test Region 4.65 eV < E (Neutron)<46.5kev.

Homogenization of the Doppler cell and hence spatial self-shielding of the cross sections was done in a cylindrical model of the Doppler cell and reactor, using the S8 transport approximation in the Program DTF IV (modified). The modification was simply the addition of a chained flux-volume weighting subroutine used to homogenize the cell, through conservation of cell reaction rates.

4.1.2 Core and Reflector Cross Sections

Core and reflector cross sections were also prepared using the Program 1DX. Heterogeneous resonance self-shielding for heavy elements in the core was again done with the Bell approximation.

The material of the core region surrounding the Doppler experiment was arranged in A and A* drawers (see Figure 7). The cell was assumed to be an A-A* drawer pair in which the plates were represented by infinite planes. As shown in Figure 15, the fuel was lumped into four regions; as ZPPR fuel plate, a SEFOR plate plus a U metal plate, a Pu metal plate plus an U metal plate and a ZPPR fuel plate plus an U_3O_8 plate. Atom densities for this approximate configuration are given in Table III. For this configuration, the heterogeneity factor is one-half the cell width or 5.542 cm.

4.1.3 Real and Adjoint Spatial Fluxes

Real and adjoint spatial fluxes for perturbation calculations (Program Pert IV) of Doppler effects were calculated with two-dimensional diffusion theory, using the program 2DB. An RZ model of Assembly 51 with the Doppler cell in the central position was calculated first. The model is described in Figure A2.

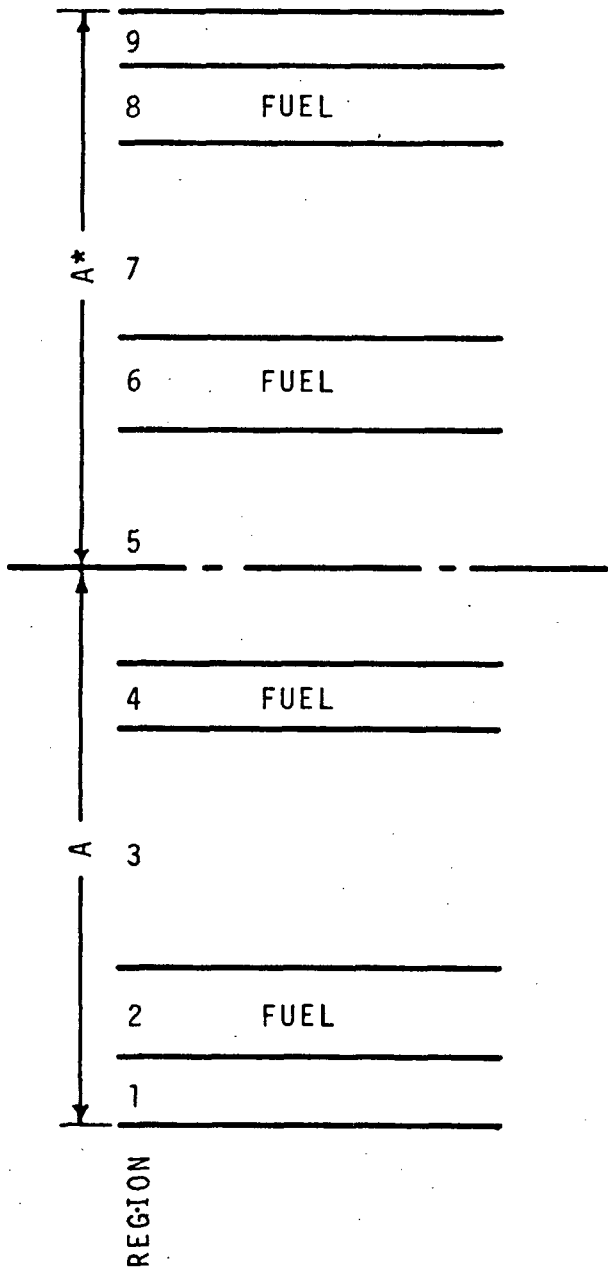

(See Table III for compositions and dimensions)

Figure 15. Unit Core Cell for Heterogeneity

TABLE III

ISOTOPIC CONCENTRATIONS IN MODEL UNIT CELL

Region	Thickness, cm	Mix	Isotope	Density, 10^{24} atom/cm^3	
1	0.723	1	C	0.004545	Coolant, clad
			Fe	0.02278	and structure
			Cr	0.005339	
			Ni	0.002336	
			Mo	0.0004782	
			Al	0.0008073	
			Na	0.013514	
			O	0.01867	
2	0.9525	2	Pu-239 + 241	0.0037544	ZPPR + U-238
			Pu-240	0.0005562	
			U-235	0.00002929	
			U-238	0.01537	
3	2.5307	1			
4	0.6338	3	Pu-239 + 241	0.012735	Pu + U-238 (metal)
			Pu-240	0.0006769	
			U-235	0.00004281	
			U-238	0.003773	
5	1.447	1			
6	0.953	4	Pu-239 + 241	0.0042037	SEFOR + U-238
			Pu-240	0.0004416	
			U-235	0.00009202	
			U-238	0.04826	
7	2.16	1			
8	0.9615	2			
9	0.7225	1			

The homogenized Doppler cell had an outer radius of 3.124 cm, the equivalent radius of a ZPR-3 matrix tube. This cell radius should not be confused with a radius of 1.75 cm, used in resonance self-shielding calculations. Atom densities for this model are those given in Table 1.

4.1.4 Normalization of Off-Center Calculations

Calculations of off-center Doppler effects were also made with two-dimensional diffusion theory using the program 2DB in the X,Y geometry mode. Again the Doppler cells were represented as homogeneous lumps. Areal profiles of the models are shown in Figures A3, A4, and A5.

Since these X,Y calculations do not model the axial nature of Assembly 51 nor that of the Doppler sample it is necessary to approximate it. This was done in the calculations with the Doppler sample in the central position, $r = 0$. The worth of U-238 per kilogram obtained from the X,Y calculation was adjusted to agree with that obtained in the corresponding R,Z calculation.

For off-center X,Y calculations this same normalization was applied. This, of course, requires the assumption that axial dependence of the real and adjoint fluxes in the resonance energy interval at $r = 22.2$, and 33.3 cm positions are the same as at $r = 0$. The only information available with respect to this question is the calculated R,Z spatial distribution of the worth of U-238 throughout the core, without the Doppler samples present. These calculations show the axial dependence at $r = 0$ and $r = 22.2$ cm to be identical. At $r = 33.3$ the variation in worth is 1% greater than at $r = 0$. Hence it is assumed that the axial variation with radius is not a source of relatively significant error in this analysis.

4.2 Experiment - Theory Comparisons

Since the Doppler reactivity changes were so small ($10^{-6}\Delta k/k$) they were obtained as differences between calculated specific Doppler sample worths at two temperatures. Perturbation theory was used to obtain specific worths of U-238 for each of 25 mesh cells throughout the Doppler cell. Volume sums yielded total Doppler cell worths for each temperature in RZ calculations for the central positions. Areal sums with the axial corrections were used for the off-center positions.

Comparisons are presented in Table IV. Here the experimental uncertainties are as given earlier. Uncertainties in the calculation are not known, therefore the uncertainties in the C/E values are due to experimental uncertainties only.

The entire set of nickel buffer experimental data and calculated values are presented graphically in Figure 16. The solid lines for each of the three temperature ranges are visual fits to the calculated results. The curves are not normalized to the experimental data. As mentioned earlier in discussions of the logarithmic fits to the data, the 300-800°K data point at r = 22.2 cm is more than two standard deviations from the calculated value. It may therefore be suspect and should perhaps not be included in an overall evaluation of this correlation.

Since visual inspection indicates that the C/E values in Table IV exhibit trends, at least with spatial position, a general statistical analysis was performed. The objective was to find, if possible, a linear relationship between calculated and experimental values and the concomitant variables temperature, position, and buffer material.

TABLE IV

ASSEMBLY 51 CALCULATED DOPPLER EFFECTS

		Reactivity Change Due to Heating from 300°K, Ih		
	T,°K	Experiment	Calculated	Calc./Exp.
r = 0	500	-0.132±0.007	-0.149	1.13±0.06
Ni Buffer	800	-0.275±0.008	-0.288	1.05±0.03
	1100	-0.386±0.009	-0.380	0.983±0.023
r = 22.2 cm	500	-0.0846±0.0066	-0.092	1.08±0.07
Ni Buffer	800	-0.152±0.007	-0.176	1.16±0.05
	1100	-0.226±0.008	-0.233	1.03±0.04
r = 33.3	500	-0.0728±0.0051	-0.065	0.898±0.06
Ni Buffer	800	-0.145±0.006	-0.125	0.863±0.04
	1100	-0.199±0.006	-0.166	0.836±0.03
r = 0	500	-0.102±0.005	-0.128	1.27±0.06
SS Buffer	800	-0.221±0.006	-0.250	1.13±0.03
	1100	-0.307±0.007	-0.332	1.08±0.02

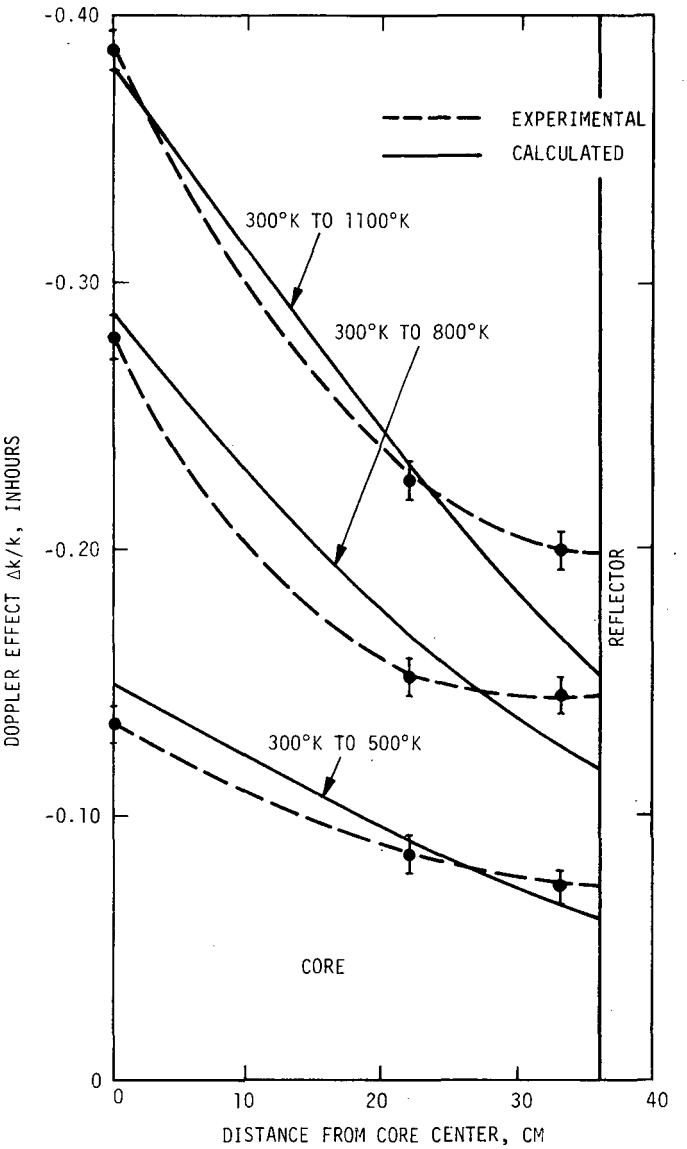

Figure 16. Assembly 51 Doppler Effects Comparisons Nickel Buffer

A general linear hypothesis program was used with the experimental data as the dependent variable and the calculated values as the independent variable. As previously stated temperature, radial position and buffer material entered as concomitant variables. The result of this analysis is an equation that predicts the experimental change given a calculated value. The analytic form is

$$\hat{y} = C(r) + D + 1.0591\ X$$

where $\hat{y}$ = predicted experimental Doppler reactivity change;

X = calculated Doppler reactivity change ;

r = radial position ;

$$D = \begin{cases} 0 \text{ for Nickel buffered experiments} \\ 0.0166 \text{ for stainless steel buffered experiments;} \end{cases}$$

$$\begin{aligned} C(0) &= 0 \\ C(22.2) &= -0.0014 \\ C(33.3) &= -0.0373. \end{aligned} \quad ;$$

The root mean square difference between the predicted experimental reactivity changes obtained from this equation and the actual experimentally inferred changes is 0.0086.

Certain properties of and comments on the calculation procedure may be made. Specifically;

1. The prediction equation has no dependence upon temperature. Hence, one may infer that the calculation procedure correctly models the effect of change of temperature. This inference is consistent with that shown early by the apparent goodness of the logarithmic fits to the experimental data. (Crystalline binding effects not evaluated in this work could alter this conclusion.)

2. Since C is dependent upon radius the calculational procedure does not correctly model the spatial dependence. If one considers the axial shape of the worth of U-238 to be invariant with radius, this model inadequacy may be taken to be a spectral problem. This has long been suspected for nickel reflected systems. This is perhaps further substantiated by the fact that D is non zero for the steel buffer. That is, the equation for prediction must differentiate between nickel and stainless steel buffers.
3. Since the root mean square value of 0.0086 is not significantly larger than the experimental uncertainties, they may be considered realistic random standard deviations.
4. Finally, the most important inference from this analysis is that the occurence of C(r) and D implies that the calculated values are systematically biased in a true statistical sense with respect to the experimental data.

In summary the spatial bias may be due to a significantly inadequate calculated spectrum at the core-reflector interface. If this is true, one may readily expect similar effects in the calculation of FTR whole core Doppler constant. Since this effect tends to be conservative for FTR, it may be of minor concern at present.

REFERENCES

1. W.R. Young and R.A. Bennett, "Analysis of FTR Phase B Critical Experiments, Part 1, ZPR-III, Assembly 51", BNWL-1138, Battelle-Northwest, Richland, Washington, January 1970.

2. W.R. Young and R.A. Bennett, "Analysis of FTR Phase B Critical Experiments, Part 2, ZPR-III, Assemblies 52 a,b,c,d,e, and f", BNWL-1139, Battelle-Northwest, Richland, Washington, January 1970.

3. J.V. Nelson and S.L. DeMyer, Group Constants (Tape U1576) for Analysis of FFTF Critical Experiments, BNWL-1044, Battelle-Northwest, Richland, Washington, March 1969.

4. I.I. Bondarenko, et. al, "Group Constants for Nuclear Reactor Calculations Consultants Bureau", New York, 1964.

5. R.A. Bennett and P.L. Hofmann, Rationale and Plans for the FTR Critical Experiments Program, BNWL-490, Battelle-Northwest, Richland, Washington, June 1967.

6. W.L. Nicholson, Battelle-Northwest, Private Communication.

7. LMFBR Liquid Metal Fast Breeder Reactor Program Plan, Vol. 9, WASH-1109 Reactor Technology, LMFBR Program Office, Argonne National Laboratory, Argonne, Illinois, August 1968.

8. Reactor Development Program Progress Report, ANL-7460, Argonne National Laboratory, Argonne, Illinois, June 1968.

9. G.J. Fischer, D.A. Meneley, R.H. Hwang, E.F. Groh, and C.E. Till, "Doppler Effect Measurements in Plutonium-Fueled Fast Power Breeder Reactor Spectra", Nuc. Sci. and Eng. Vol. 25, p. 37, 1966.

10. R.A. Lewis and T.W. Johnson, "Sensitivity of Small-Sample Doppler Effect Measurements to Environment", ANL 7410, Argonne National Laboratory, Argonne, Illinois, p. 96, 1969.

11. R.N. Hwang and L. Miller, "Monte Carlo Calculations of Multi-Region Hot-Cold Interference Effects", ANL 7410, Argonne National Laboratory, Argonne, Illinois, p. 110, October 1966.

12. R.W. Hardie and W.W. Little, Jr., "1DX, A One-Dimensional Diffusion Code for Generating Effective Nuclear Cross Sections", BNWL-954, Battelle-Northwest, Richland, Washington, March 1969.

13. DTF-IV (modified) is a BNWL version of DTF-IV, K.D. Lathrop, "DTF-IV, A Fortran IV Program for Solving the Multigroup Transport Equation with Anisotopic Scattering", LA-3373, Los Alamos Scientific Laboratory, Los Alamos, New Mexico, July 15, 1965.

14. W.W. Little, Jr., and R.W. Hardie, "2DB, A Two-Dimensional Diffusion Burnup Code for Fast Reactor Analysis", BNWL-640, Battelle-Northwest Richland, Washington, January 1968.

REFERENCES CONT.

15. R. W. Hardie and W. W. Little, Jr., "PERT-IV, A Two-Dimensional Perturbation Code in FORTRAN-IV", BNWL-409, Battelle-Northwest, Richland, Washington, April 1967.

16. G. I. Bell, "A Simple Treatment for Effective Resonance Absorption Cross Sections in Dense Lattices", Nuc. Sci., and Eng., Vol. 5, p. 138, 1959.

APPENDIX A

Calculational Models

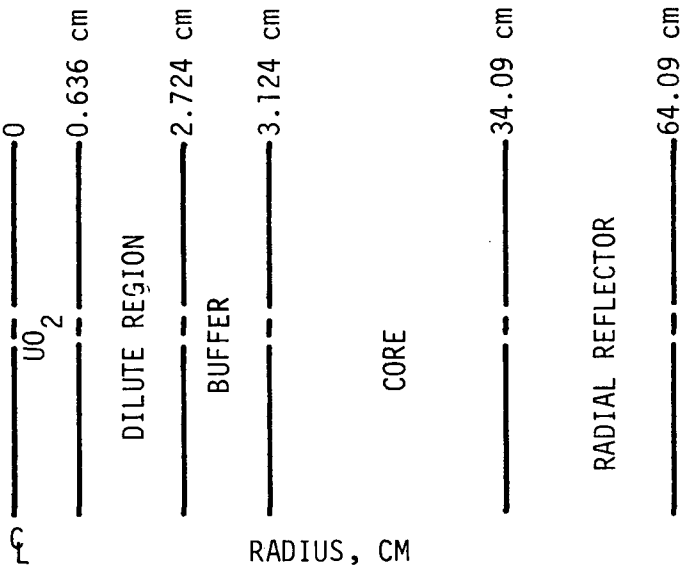

Figure A-1. Cylindrical Doppler Element Cell Calculation Model.

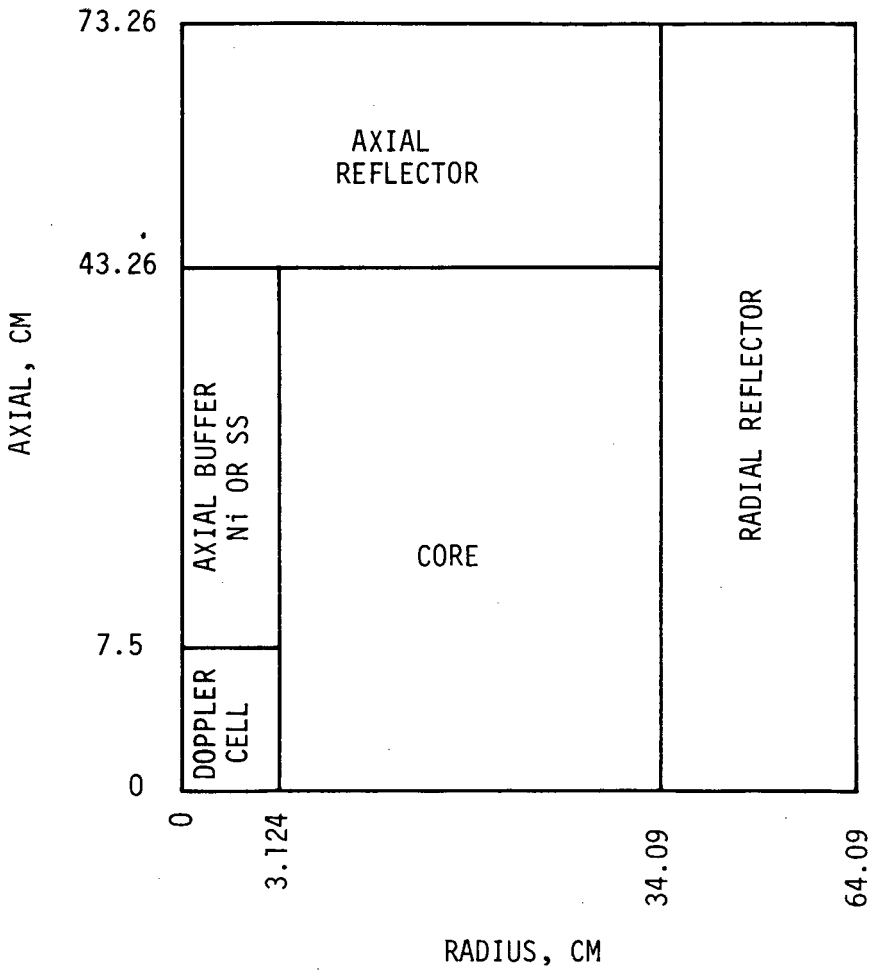

Figure A-2. RZ Reactor Model for Flux and Adjoint. Central Measurement.

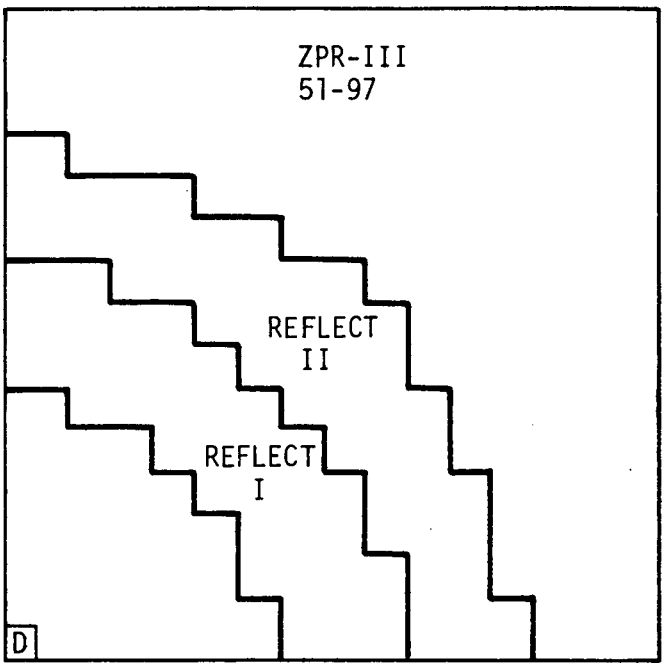

D DOPPLER CELL

AXIAL BUCKLING = 0.000682 cm^{-2}

K = 0.9832

R = 0 cm

Figure A-3. X-Y Reactor Model for Flux and Adjoint. Central Measurement.

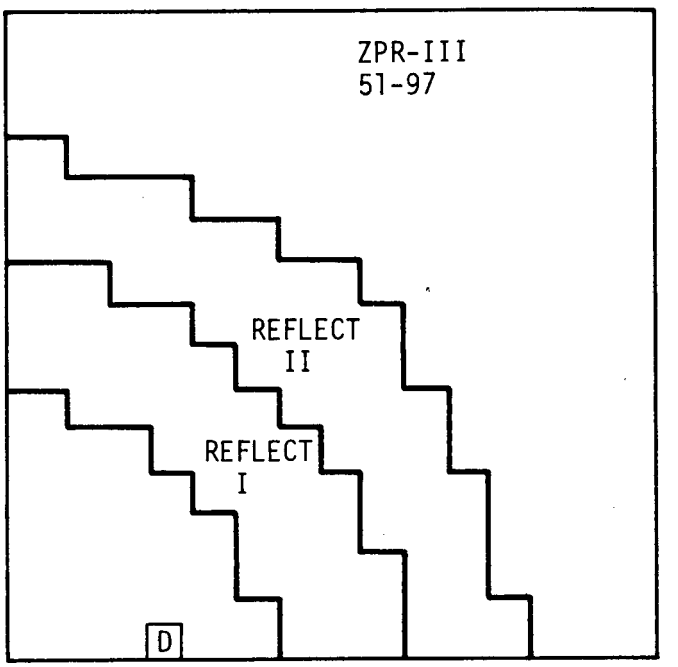

D DOPPLER CELL

AXIAL BUCKLING = 0.000682 cm^{-2}

K = 0.9819

R = 22.2 cm

Figure A-4. X-Y Reactor Model for Flux and Adjoint. r = 22.2 cm.

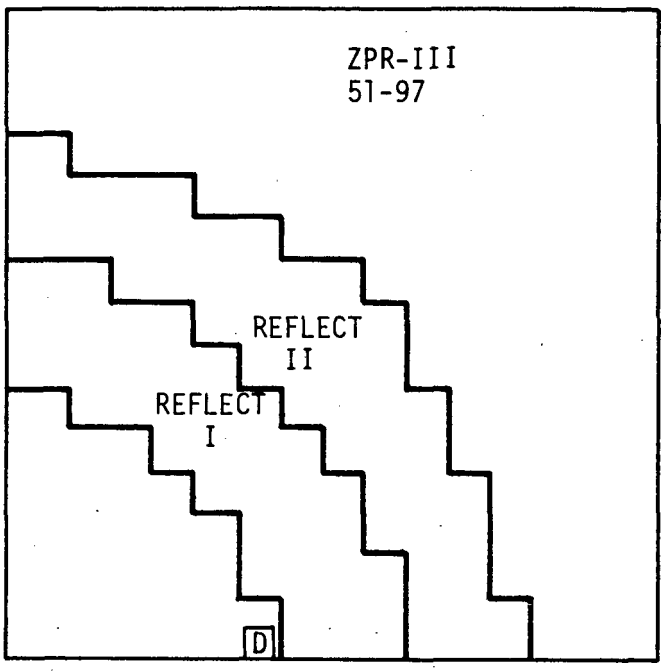

D DOPPLER CELL

AXIAL BUCKLING = 0.000682 cm^{-2}

K = 0.9897

R = 33.3 cm

Figure A-5. X-Y Reactor Model for Flux and Adjoint. r = 33.3 cm.